ELSEVIER

Biophysical Chemistry 129 (2007) 289–297

Biophysical Chemistry

http://www.elsevier.com/locate/biophyschem

Kinetics of binding the mRNA cap analogues to the translation initiation factor eIF4E under second-order reaction conditions

Elżbieta Błachut-Okrasińska, Elżbieta Bojarska, Janusz Stępiński, J.M. Antosiewicz *

Department of Biophysics, Warsaw University, Żwirki i Wigury 93, 02-089 Warszawa, Poland

Received 10 May 2007; received in revised form 20 June 2007; accepted 25 June 2007
Available online 3 July 2007

Abstract

The kinetics of binding of five analogues of the 5′-mRNA cap, differing in size and electric charge, to the eukaryotic initiation factor eIF4E, at 20 °C, pH 7.2, and ionic strength of 150 mM, were measured, after mixing solutions of comparable concentrations of the reagents, in a stopped-flow spectrofluorimeter.

The registered stopped-flow signals were fitted using an efficient software package, called Dyna Fit, based on a numerical solution of the kinetic rate equations for assumed reaction mechanisms. One-, two-, and three-step binding models were considered. The quality of fits for these models were compared using two statistical criteria: Akaike's Information Criterion and Bayesian Information Criterion. Based on resulting probabilities of the models, it was concluded that for all investigated ligands a one-step binding model has essentially no support in the experimental observations.

Our conclusions were also analysed from the perspective of kinetic transients obtained for cap–eIF4E systems under the so called pseudo-first order reaction condition, which result in the linear correlation of the observed association rate constant with ligand concentration. The existence of such a linear correlation is usually considered as proof of a one-step binding mechanism. The kinetic and optical parameters, derived from fitting a two-step cap-binding model with the DynaFit, were used to simulate kinetic transients under pseudo-first order reaction conditions. It appeared that the observed association rate constants derived from these simulated transients are also linearly correlated with the ligand concentration. This indicated that these linear dependencies are not sufficient to conclude a one-step binding.

Keywords: eIF4E; 5′-mRNA cap; Binding; Kinetics; DynaFit

1. Introduction

Eukaryotic mRNAs possess a cap structure consisting of a 5′-5′-tri-phosphate bridge of a general form m^7GpppN^1, where m^7G is the 7-methyl-guanosine, and N can be any of the four nucleosides [1]. One of the essential steps in the initiation of eukaryotic mRNA translation is the recognition of this cap structure by a eukaryotic initiation factor 4E (eIF4E) [2]. The protein eIF4E is a part of a trimeric complex, termed eIF4F, which also contains an adaptor protein eIF4G and RNA helicase eIF4A [3]. The crucial element of the cap recognition consists of sandwiching of the alkylated base between the side chains of two conserved tryptophans (Trp-56 and Trp-102 in the murine eIF4E). The interaction can be explained in terms of enhancement of π–π stacking enthalpy, because of charge transfer between the electron-deficient 7-methylguanine (which carries a delocalised positive charge secondary to methylation) and the electron-rich indole groups. Moreover there is a number of hydrogen bonds stabilising the complex, N1 and N2 make hydrogen bonds with the carboxylate oxygen atoms of Glu103, and Arg157 and Lys162 make such contacts with oxygen atoms of the phosphate groups. Many of these hydrogen bonding interactions include contributions due to direct electrostatic interactions because the interacting groups are ionised. The interaction energies also include contributions due to shifts in the appropriate pK_a values upon binding. These insights into structural characteristics of cap–eIF4E complexes were obtained from three-dimensional structures by X-ray crystallography

Abbreviations: G, guanosine; m^7G, 7-methyl-guanosine; ppp, 5′-5′-tri-phosphate bridge; GMP (GDP, GTP), guanosine 5′-mono-(di-tri-)-phosphate; eIF4E, eukaryotic initiation factor 4E.

* Corresponding author. Tel.: +48 22 554 0786; fax: +48 22 554 0771.
E-mail address: jantosi@biogeo.uw.edu.pl (J.M. Antosiewicz).

0301-4622/$ - see front matter © 2007 Elsevier B.V. All rights reserved.
doi:10.1016/j.bpc.2007.06.009

[4–6] and multi-dimensional NMR study [7], as well as from spectroscopic investigations in vitro, both equilibrium [5,8,9], and kinetic [10–14].

The reported kinetic studies were based on transient fluorescence measured in stopped-flow spectrometers. Kinetic methods allow direct measurement of rate constants governing individual steps of molecular processes. One of the issues considered in the kinetic studies was the consideration of the most appropriate model for the mechanism of cap binding by the protein initiation factor.

The simplest receptor–ligand binding model is a one-step mechanism written as

$$P + L \underset{k_D}{\overset{k_R}{\rightleftharpoons}} K. \tag{1}$$

In principle, however, when a protein binds a single ligand molecule, some rearrangement of the protein–ligand complex following the initial collision can be expected, which leads to a two-step binding kinetics [15], described by

$$P + L \underset{k_{-1}}{\overset{k_{+1}}{\rightleftharpoons}} C \underset{k_{-2}}{\overset{k_{+2}}{\rightleftharpoons}} K. \tag{2}$$

It can also happen that the association process is best described by a distribution of many relaxations, in such case one can expect that a three-step or even a multi-step model is the best way to describe protein–ligand association. Here we will consider three-step association as the most complex model:

$$P + L \underset{k_{-1}}{\overset{k_{+1}}{\rightleftharpoons}} C \underset{k_{-2}}{\overset{k_{+2}}{\rightleftharpoons}} D \underset{k_{-3}}{\overset{k_{+3}}{\rightleftharpoons}} K. \tag{3}$$

In the above equations, k_i are the appropriate rate constants, C and D represent intermediate forms and K represents the final form of the complex of protein P and ligand L.

One of the important aspects of investigating the receptor–ligand association reactions by stopped-flow spectrometry is that the initial state of an investigated system, at the moment of the reagent mixing, can be arbitrary far from the thermodynamic equilibrium achieved during the course of the initiated reaction. Therefore, data analysis is more complicated than in the case of the so called relaxation methods. In the past, this led to restrictions to simplified reaction schemes and/or experiments designs. A classical example in this respect is performing stopped-flow experiments under the so called pseudo-first order reaction conditions, where the concentration of one component is much higher than the concentration of the other reagent. Under these conditions, the rate equations can be integrated to yield mono-exponential time dependence of the concentration of reactants [15]. The observed F signal is also a mono-exponential function of time

$$F(t) = F_\infty + (F_o - F_\infty) \cdot \exp(-k_{\text{obs}} t) \tag{4}$$

where k_{obs} is the observed first-order rate constant, and F_o and F_∞ is the initial and final signal, respectively, registered for the solution. Analysis of k_{obs} versus total ligand concentration can be used to distinguish between the one-step and two-step association mechanism for ligand binding [15–19].

For a one-step mechanism k_{obs} is a linear function of the total ligand concentration $[L]$

$$k_{\text{obs}} = k_R[L] + k_D. \tag{5}$$

For the above two-step binding mechanism, and ligand concentrations much larger than the protein concentration, the steady-state assumption and the condition that $[C]=[K]=0$ at time zero, the observed rate constant reads [16–18]

$$k_{\text{obs}} = \frac{k_{+1}[L](k_{+2} + k_{-2}) + k_{-1}k_{-2}}{k_{+1}[L] + k_{-1} + k_{+2}}. \tag{6}$$

Assuming that $k_{-1} \gg k_{+2}$, the last equation can be simplified to a hyperbolic dependence

$$k_{\text{obs}} - k_{-2} = \frac{k_{+1}k_{+2}[L]}{k_{+1}[L] + k_{-1}} \tag{7}$$

which, by neglecting k_{-2}, can be also presented as a linear relation between the inverse of the observed rate constant and the inverse of the ligand concentration. The hyperbolic saturation phenomenon of k_{obs} as a function of the total ligand concentration $[L]$ is commonly considered as an indication of more than one step in the protein–ligand binding mechanism [15–18]. According to Eq. (7), at some high concentration of the ligand, the observed rate is limited by first-order isomerisation of the protein–ligand complex, i.e. $k_{+2}+k_{-2}$ [15].

Advances in computational methods to analyse reaction time courses by numerical integration [19–21] removed the necessity to restrict data analysis to simplified reaction schemes and/or particular design of the experiments. Particularly useful for numerical analysis of transient kinetic signals registered in stopped-flow spectrometers is the DynaFit program developed by Petr Kuzmic [21]. With this program one can fit a postulated theoretical model to given experimental data or one can simulate pseudo-experimental data.

A considered reaction model can be fit simultaneously to several sets of experimental data, e.g. several kinetic transients registered for different initial concentrations of the reagents. When several transients are analysed simultaneously within restrictions imposed by a particular reaction mechanism, a larger number of model parameters might be reliably determined from data fitting. The program allows for a discrimination analysis of various models which results in a statistically justified choice of the most appropriate reaction scheme for a given system.

Stopped-flow investigations of the binding of m^7GpppG to eIF4E protein, under pseudo-first order reaction conditions, were performed by Goss and coworkers [10,13] and by Slepenkov and coworkers [14]. The first group concluded that the binding is a two-step process and according to the second group a one-step reaction is sufficient to describe experimental data. Our group investigated the association of eIF4E protein with cap analogues using stopped-flow spectrofluorimetry under secondary-reaction conditions [11,12]. In the earlier study we have used mono- and bi-exponential functions in experimental data fitting and the obtained rate constants were interpreted in terms of plausible one-

and two-step association mechanisms. In the second study we used a home written software similar to the DynaFit program but designed only for one-step and two-step association mechanisms, and lacking sophisticated statistical analysis tools implemented in the latter. Therefore, in the present study we decided to use the DynaFit software.

The aim of the present work is to apply stopped-flow spectrofluorimetry to determine the rate constants for complex formation between eIF4E and five cap analogues: m^7GMP, m^7GDP, m^7GTP, m^7GpppG, m^7Gpppm^{7}G, to analyse the experimental observations in terms of a one-, two- or three-step protein–ligand binding models, and to compare probabilities of these models based on a discrimination analysis approach implemented in the DynaFit program namely Akaike's Information Criteria (AIC) [22,23]. As a second method for statistical analysis the Bayesian Information Criterion [24,23] was used. Based on the probabilities for the models described by Eqs. (1)–(3), derived from AIC parameters, we conclude that one-step binding model for association of cap analogues with eIF4E protein has no support in the stopped-flow kinetic transients. Thus the binding is at least a two-step process.

2. Materials and methods

2.1. Reagents, syntheses, and protein preparation

m^7GMP, m^7GDP and m^7GTP were synthesised from GMP, GDP and GTP (purchased from Sigma Co.), and converted prior to use into their triethylammonium salts, as described elsewhere [25–27]. Dinucleoside cap analogues (m^7GpppG and m^7Gpppm^{7}G) were prepared according to [28].

Murine eIF4E (28–217) was expressed in *E. coli*, strain BL21(DE3)pLysS, transformed with a pET 11d plasmid. The cultures of bacteria were grown in Luria–Berthani broth with ampicillin and chloramphenicol until $OD_{595\ nm}$ about 1.0 when IPTG was added (0.5 mM) to induce T7 polymerase. The protein was purified from inclusion bodies pellet and folded by one-step dialysis from 6 M GdmHCl, followed by anion exchange chromatography on a MonoS column [4].

2.2. Stopped-flow measurements

The binding of cap analogues to eIF4E can be followed by measurements of quenching of intrinsic tryptophan fluorescence of eIF4E, see e.g. [8], due to sandwich stacking between 7-methylguanine and two tryptophan indole rings [4,7]. Measurements were done using a SX.18MV stopped-flow reaction analyser from Applied Photophysics Ltd. The investigated association processes were initiated by mixing equal volumes of defined concentrations of eIF4E (1.0 μM) and a cap analogue (between 0.25 and 8.0 μM, depending on the ligand), at 20 °C, ionic strength of 150 mM, and pH 7.2, in 50 mM Hepes–KOH buffer. Concentrations of the reagents were determined spectrophotometrically as described previously [12]. Optical parameters for unbound states of the protein and ligands were obtained from measurements with solutions containing only single reagent, for the same stopped-flow apparatus setup as used in the binding measurements. For each cap analogue, 4 to 5 different concentrations were used in one set of experiments. Each registered kinetic transient is an average of 8 to 12 shots. All solutions were filtered and degassed prior to the measurements. For each combination of protein and ligand concentrations, the set of experiments was repeated 3 times with protein samples from separate preparations. It should be noted that eIF4E protein is a difficult system to study because of problems with the preparation of stable and fully active samples of eIF4E protein, as discussed previously [5,11,14].

2.3. Analysis of the experimental data

At any given moment of time the fluorescence of the solution can be represented as a sum of contributions due to distinguishable molecular species in the mixture, i.e. the free protein and ligand molecules, and one or more forms of their complex:

$$F(t) = \sum_x F_x \cdot c_x(t) \tag{8}$$

where c_x is the molar concentration of molecular species X and F_x is its "molar fluorescence" for given solution conditions and the spectrofluorimeter settings. Eq. (8), together with the integration of the kinetic differential equations appropriate for the mechanism of association described by Eqs. (1)–(3), allows one to determine the values of the kinetic and optical parameters characterising the molecular species. These tasks were performed by the DynaFit program [21] using script files of the form presented in Ref. [29].

The model discrimination analysis in the DynaFit program employs the second-order Akaike's Information Criteria parameters [30] described by

$$\mathrm{AIC} = n \log \frac{\mathrm{RSS}}{n} + 2k + \frac{2k(k+1)}{n-k-1} \tag{9}$$

where n represents the number of experimental data points, k is the number of adjustable parameters and RSS is the residual sum of squares from the estimated model. Eq. (9) is a valid expression for the AIC parameters in the case of least squares estimation and normally distributed errors [23]. Performing the model selection, one finds the lowest second-order $\mathrm{AIC}^{\min}$ among the considered models, and AIC differences

$$\Delta\mathrm{AIC}_i = \mathrm{AIC}_i - \mathrm{AIC}^{\min} \tag{10}$$

where i enumerates models. $\Delta\mathrm{AIC}_i$s are subsequently used to determine the Akaike's weights indicating probabilities of different models:

$$w_{\mathrm{AIC},i} = \frac{\exp(-0.5 \cdot \Delta\mathrm{AIC}_i)}{\sum_{r=1}^{R} \exp(-0.5 \cdot \Delta\mathrm{AIC}_r)} \tag{11}$$

where R is the number of models taken into consideration. The first term on the right hand side of Eq. (9) represents the lack of fit measure and the sum of the second and third terms represents

the model complexity measure [23]. This sum penalises complex models. In our case the penalty term practically equals $2k$, as the number of experimental data points is always above 3000, and the number of parameters does not exceed 17 (in the present study this is the value for four-step model). Moreover, a consequence of the large number of experimental data points is that relatively small improvements in the RSS, when the number of adjustable parameters is increased, result in a significant decrease of the first term in Eq. (9), which can easily surmount an accompanying increase in the penalty term. One might then expect that the AIC approach can lead to unjustified favouring of models with too large number of adjustable parameters. Therefore, it might be useful to look at our models using another measure of generalisability which achieves a balance between quality of fit and complexity, and penalises the increasing number of parameters more than the AIC does. For this purpose we have chosen the Bayesian Information Criterion (BIC) approach [24,23]. Again, for least squares estimation and normally distributed errors, the formula for the BIC is

$$\mathrm{BIC} = n \cdot \log \frac{\mathrm{RSS}}{n} + k \cdot \log(n). \tag{12}$$

Given any two estimated models, the model with the lower value of the BIC is the preferred one. As in the case of the AIC, one computes the BIC for each model, $\Delta\mathrm{BIC}_i$s are defined as the difference of the BIC for model i and the minimum BIC value, and the BIC weights are calculated, which indicate probabilities of different models:

$$w_{\mathrm{BIC},i} = \frac{\exp(-0.5 \cdot \Delta\mathrm{BIC}_i)}{\sum_{r=1}^{R} \exp(-0.5 \cdot \Delta\mathrm{BIC}_r)}. \tag{13}$$

Expression for the BIC is similar to that for the AIC except that it gives greater weight to simplicity by a factor of $\log(n)/2$.

3. Results and discussion

3.1. Kinetic transients from stopped-flow experiments

Fig. 1 shows examples of kinetic traces obtained after mixing equal volumes of 1 μM solution of the eIF4E protein and the solution of each of the five cap analogues. The observed signal decay results from the protein's tryptophan fluorescence quenching accompanying the formation of the complex [8]. It can be noted that quenching is the smallest and slowest for m^7GMP, and the largest and fastest for m^7GTP, and that with an increasing concentration of the ligand, a smaller part of the binding reaction is visible in the kinetic traces. For example, for m^7GTP, for the concentration exceeding 5 μM in the stopped-flow syringe, the whole binding reaction is completed within the dead-time of the instrument.

The first step of analysis of the kinetic transients registered in this study was to fit them assuming one-, two-, or three-step binding mechanisms of eIF4E and cap analogues, using the DynaFit program. Table 1 shows rate constants and optical

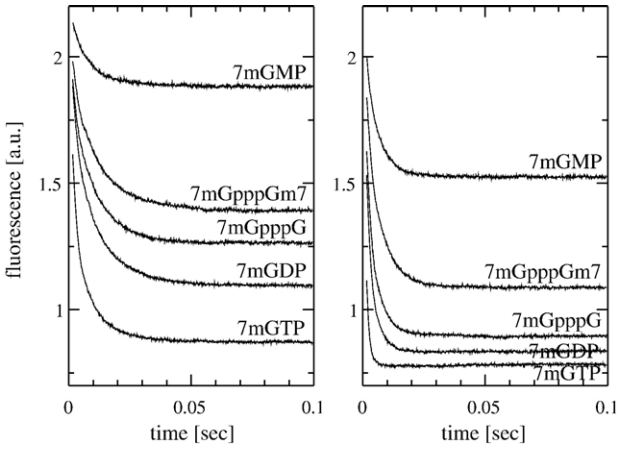

Fig. 1. Examples of kinetic traces obtained after mixing equal volumes of 1 μM solution of eIF4E with 1 μM (left side) and with 3 μM (right side) solutions of the indicated cap analogues.

parameters resulting from fitting the one-step mechanism, for each of the three sets of traces registered in independent experiments, and for all cap analogues investigated in this work. Additionally, Table 1 presents the resulting average association equilibrium constants, $K_a = k_R/k_D$. These association constants remain in good agreement with the results of equilibrium fluorescence titration measurements described by Niedźwiecka and coworkers [5]. Optical properties of the complexes are given as relative quantities, taking the fluorescence of 1 μM solution of the eIF4E protein as a unit.

In the fittings described here all appropriate for a given binding mechanism rate constants and optical parameters as well as offset levels were used as adjustable parameters. In order to check the importance of other parameters on the results of the fitting procedure some other parameters were also considered as adjustable, like protein and ligand concentrations or optical parameters for the free reagents. In particular, when the protein concentration was used as an adjustable parameter the final values resulting from the fittings remained within 10% of the initial value and the shifts from this value were apparently accidental. Therefore, in the results reported here the total concentration of the protein was kept constant 0.5 μM, as was determined spectrophotometrically.

A comparison of the rate constants, resulting from fitting the one-step model to experimental data, with our previous results [12] shows that the results for m^7GMP for pH of 7.2 are similar, whereas regarding m^7GDP and m^7GTP, in the earlier study we obtained somewhat lower association and higher dissociation rate constants, respectively. It can result from lower activity of protein samples obtained in the previous preparations. Average association rate constant for m^7GpppG, $k_R = 191 \pm 6$ [$\mu M^{-1}\ s^{-1}$] is not much different from the value obtained by Slepenkov et al. for the same ligand but with human eIF4E protein [14]. These authors obtained 184 ± 10 [$\mu M^{-1}\ s^{-1}$] for 100 mM of KCl added to the solution, and 102 ± 7 [$\mu M^{-1}\ s^{-1}$], for 150 mM KCl. The ionic strength of each of these solutions is about 15 mM higher because of the contribution of the buffer components. On the other hand, our dissociation rate constant,

Table 1
Results of one-step model fitting to the kinetic transients

Experiment no.	Parameter	Cap analogue				
		m^7GMP	m^7GDP	m^7GTP	m^7GpppG	m^7Gpppm^{7}G
I	k_R	69.9	246.	743.	191.	161.
	k_D	87.7	11.8	7.35	24.5	24.4
	F_K	0.41	0.45	0.35	0.41	0.44
II	k_R	68.7	278.	672.	188.	138.
	k_D	94.3	12.7	9.57	21.9	26.1
	F_K	0.38	0.39	0.38	0.42	0.42
III	k_R	71.7	291.	666.	194.	119.
	k_D	84.9	10.0	10.4	20.7	24.4
	F_K	0.48	0.45	0.37	0.47	0.51
	K_a	0.79±0.12	23.9±9.0	78.4±39.7	8.58±1.58	5.59±1.80

The equilibrium association constants are averages of the three values resulting from the ratio k_R/k_D, and their errors are double standard deviations of the average value. The association rate constants, k_R, are given in units of [μM^{-1} s^{-1}], the dissociation rate constants, k_D, in [s^{-1}], and the equilibrium association constants, K_a in [μM^{-1}]. The contribution of the complex to the measured fluorescence signal is relative to the signal of the free protein.

k_D=22.4±3.9 s^{-1}, is about 4 times smaller than the values reported by these authors for similar amounts of added KCl, but it should be noted that the way of derivation of k_D from experimental data is different. So we can conclude that assuming the one-step binding we obtain results comparable to other researchers who analysed their data also assuming the one-step binding, and this indicates that the quality of our experimental data is satisfactory.

Table 2 shows rate constants and optical parameters resulting from fitting the two-step mechanism by the DynaFit program, and Fig. 2 presents two examples of kinetic traces obtained after the mixing of solutions of the eIF4E and two of the five cap analogues used in this work, m^7GMP and m^7GpppG, respectively, together with the theoretical transients, resulting from fitting the two-step binding model to the experimental traces. Additionally Table 2 presents the resulting overall average association equilibrium constants, computed according to [31]

$$K_{a,\text{overall}} = \frac{k_{+1}}{k_{-1}}\left(1+\frac{k_{+2}}{k_{-2}}\right).$$

It can be noted that the rate constants and optical parameters resulting from fitting the two-step binding mechanism vary for each ligand more among independent sets of experiments than those resulting from one-step fitting. However, despite the larger variation of the values of the rate constants obtained from fitting the two-step model, overall association constants remain in semi-quantitative agreement with the results obtained for the one-step model. Moreover, parameters derived from the two-step fitting exhibit another kind of consistency, namely, they all, when used in

Table 2
Results of two-step model fitting to the kinetic transients

Experiment no.	Parameter	Cap analogue				
		m^7GMP	m^7GDP	m^7GTP	m^7GpppG	m^7Gpppm^{7}G
I	k_{+1}	72.3	225.	769.	203.	165.
	k_{-1}	127.	58.9	20.7	44.0	33.5
	k_{+2}	19.6	201.	68.0	30.4	12.8
	k_{-2}	82.4	102.	72.1	74.2	58.7
	F_C	0.26	0.07	0.29	0.34	0.40
	F_K	0.50	0.43	0.31	0.38	0.44
II	k_{+1}	72.4	239.	653.	196.	149.
	k_{-1}	169.	62.9	54.4	63.8	62.0
	k_{+2}	74.7	182.	119.	65.7	72.0
	k_{-2}	175.	106.	68.4	72.4	94.9
	F_C	0.11	0.01	0.19	0.26	0.30
	F_K	0.48	0.38	0.29	0.37	0.38
III	k_{+1}	80.6	241.	525.	192.	139.
	k_{-1}	111.	45.9	95.1	68.6	65.3
	k_{+2}	7.15	207.	206.	121.	76.9
	k_{-2}	71.7	131.	76.8	101.	84.5
	F_C	0.43	0.08	0.01	0.28	0.42
	F_K	0.36	0.47	0.30	0.45	0.45
	$K_{a,\ \text{overall}}$	0.70±0.09	11.7±1.7	41.8±27.1	6.16±0.32	4.89±1.12

The association rate constants, k_{+1}, are given in units of [μM^{-1} s^{-1}], the remaining rate constants are given in [s^{-1}]. The contribution of the complexes to the measured fluorescence signal is relative to the signal of the free protein.

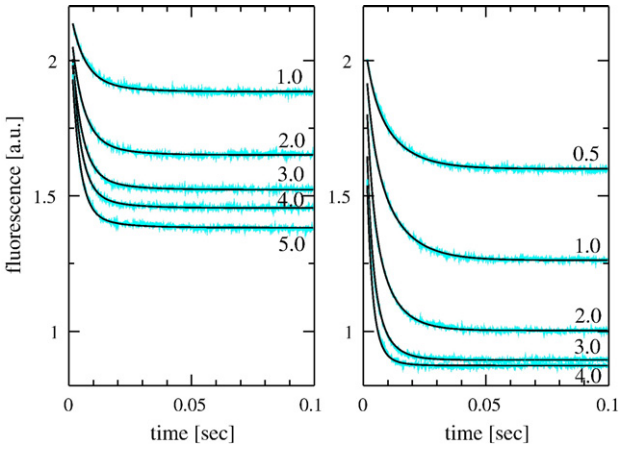

Fig. 2. Examples of kinetic traces (noisy lines) obtained after mixing equal volumes of 1 μM solution of eIF4E with solutions of m^7GMP (left side, concentrations 1, 2, 3, 4, and 5 μM), and with solutions of m^7GpppG (right side, concentrations of 0.5, 1, 2, 3, and 4 μM). Smooth black lines represent simultaneous fitting of predicted transients to the experimental data, according to a two-step association model represented by Eq. (2), by the DynaFit program.

the simulation of kinetic transients under pseudo-first order reaction condition, predict a linear dependence of the k_{obs} on ligand concentration [L] in the range accessible for stopped-flow measurements. This will be discussed in the last section.

The larger variation in the values of the rate constants in the two-step model most probably results from the problems related to the sample stability mentioned in the Material and methods section and it might be difficult to overcome these difficulties. It is obvious that even if the binding is really a two- or three-step process, obtaining stable values of the parameters, from fittings for independent experiments, requires an increasingly better quality of experimental data with an increasing number of adjustable parameters. The variation of the parameter values among independent experiments observed in Table 2 is one of the reasons that although the three- and four-step binding models were also fitted to the kinetic traces, the resulting parameters are not shown. Another reason is specified in the next section.

Looking at the rate constants presented in Tables 1 and 2 one can notice a strong variance of both the association and dissociation rate constants among the ligands. The ratio of about 10 between the largest and the lowest value is observed. The rate constants roughly correlate with the total electric charge of the analogues: for the largest charge the association constant is the largest and the dissociation constant is the lowest. For the ligand with the lowest charge this is just opposite. The large differences observed in experiments make the eIF4E–cap system an interesting model system for theoretical analysis, e.g. analysis of diffusional encounter rate constants by Brownian dynamics simulation methods. Obtaining reliable diffusional association protein–ligand binding constants, and using them in two-step model analysis of the experimental kinetic traces, might be helpful in achieving better consistency of the parameter values derived from the fitting.

3.2. Discrimination between one-step and two-step binding models for eIF4E–cap systems

For all kinetic traces obtained in the present work, the model discrimination analysis tool, based on the Akaike's Information Criterion approach, implemented in the DynaFit program indicated that a one-step binding model has essentially no support in the experimental data. This conclusion is obtained when only one-step and two-step association models are taken into account, as well as when models with a larger number of steps (up to 4 were checked) are included. Table 3 shows details of this analysis for one experiment for each ligand, and Fig. 3 shows the Akaike's weights for the three models resulting from the analysis of all experiments done in the present work. For all cases the probability of a one-step binding model is zero.

Table 3
Model discrimination analysis for binding 5 cap analogues by eIF4E protein, using Akaike's Information Criteria approach, for experiment no. I (see Tables 1 and 2)

Association model	Parameter	Cap analogue				
		m^7GMP	m^7GDP	m^7GTP	m^7GpppG	m^7Gpppm^{7}G
1-step	n	4900	4900	4840	4900	4900
	k	8	8	8	8	8
	RSS	0.1646	0.3708	0.1824	0.2504	0.2408
	$\triangle AIC_i$	2734.	2214.	351.3	4486.	2919.
	w_i	0.0000	0.0000	0.0000	0.0000	0.0000
2-step	n	4900	4900	4840	4900	4900
	k	11	11	11	11	11
	RSS	0.0941	0.2357	0.1695	0.1070	0.1521
	$\triangle AIC_i$	0.0	0.0	0.0	325.9	676.2
	w_i	0.9641	0.9512	0.8585	0.0000	0.0000
3-step	n	4900	4900	4840	4900	4900
	k	14	14	14	14	14
	RSS	0.0941	0.2357	0.1694	0.1000	0.1324
	$\triangle AIC_i$	6.578	5.939	3.605	0.0	0.0
	w_i	0.0359	0.0488	0.1416	1.0000	1.0000

The one-, two- and three-step binding models are presented by Eqs. (1)–(3). Parameter's column refers to the variables used in model discrimination analysis: n is the number of data points, k is the number of adjustable parameters, RSS is the residual sum of squares (rounded to four significant digits), the $\triangle AIC_i$ is the difference between AIC_c for a given model and the lowest AIC_c among all models, the weights w_i are determined by Eq. (11).

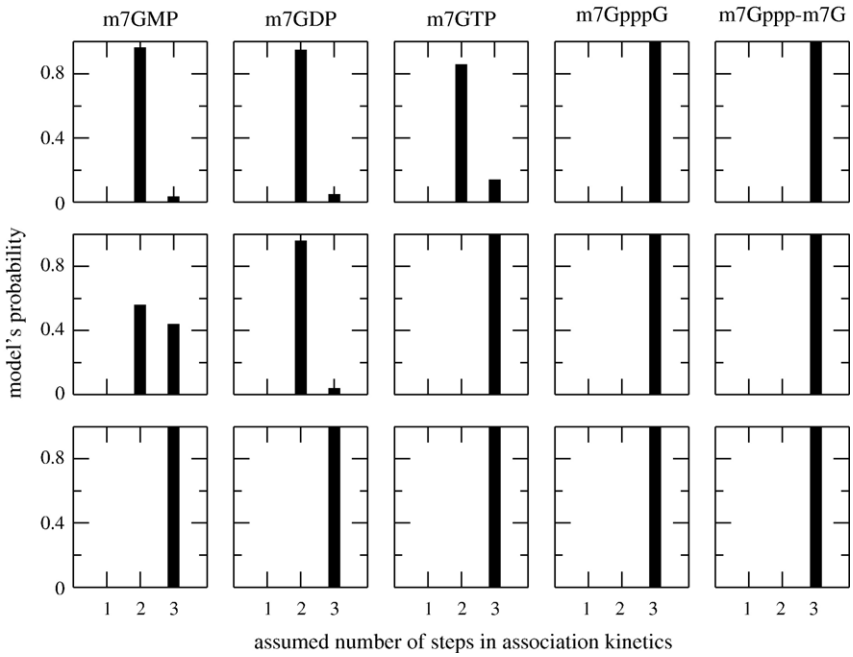

Fig. 3. Probabilities of different models for association of cap analogues with eIF4E protein according to Akaike's Information Criteria approach. The results shown in the first row correspond to data shown in Table 3.

Moreover, it can be seen that the maximum probability is shifted towards models with more steps when the size of the ligand is increasing. So for dinucleotide ligands, models with three association steps are indicated as the most probable. In this work however, we do not provide rate constants resulting from fitting models with more than two steps because the confidence intervals of the best-fit values for some of the adjustable parameters in models with more than two steps are very wide and this justifies that at least at the present state of our study such models should be rejected. Moreover, for both one- and two-step binding models confidence intervals estimated by the DynaFit program are narrow.

Table 4 shows details of the application of the Bayesian Information Criterion analysis for the same experiment for each ligand as presented in Table 3. It can be seen that despite the larger penalty of increasing the number of parameters in the considered models, the results of the Bayesian Information Criterion analysis are basically the same as those of the AIC approach.

3.3. Linear dependence of k_{obs} on [L] is not sufficient to conclude one-step binding

As was noted above, the kinetics of binding of m^7GpppG to eIF4E protein was already investigated by Goss and coworkers

Table 4
Model discrimination analysis for binding 5 cap analogues by eIF4E protein, using Bayesian Information Criteria approach, for experiment no. I (see Tables 1 and 2)

Association model	Parameter	Cap analogue				
		m^7GMP	m^7GDP	m^7GTP	m^7GpppG	m^7Gpppm^{7}G
1	n	4900	4900	4840	4900	4900
	k	8	8	8	8	8
	RSS	0.1646	0.3708	0.1824	0.2504	0.2408
	$\triangle BIC_i$	2715.	2195.	331.9	4447.	2880.
	w_i	0.0000	0.0000	0.0000	0.0000	0.0000
2	N	4900	4900	4840	4900	4900
	K	11	11	11	11	11
	RSS	0.0941	0.2357	0.1695	0.1070	0.1521
	$\triangle BIC_i$	0.0	0.0	0.0	306.5	656.8
	w_i	1.0000	1.0000	1.0000	0.0000	0.0000
3	N	4900	4900	4840	4900	4900
	K	14	14	14	14	14
	RSS	0.0941	0.2357	0.1694	0.1000	0.1324
	$\triangle BIC_i$	26.03	25.39	23.03	0.0	0.0
	w_i	0.0000	0.0000	0.0000	1.0000	1.0000

The one-, two- and three-step binding models are presented by Eqs. (1)–(3). Parameter's column refers to variables used in model discrimination analysis: n is the number of data points, k is the number of adjustable parameters, RSS is the residual sum of squares (rounded to four significant digits), the $\triangle BIC_i$ is the difference between BIC for a given model and the lowest BIC among all models, the weights w_i are determined by Eq. (13).

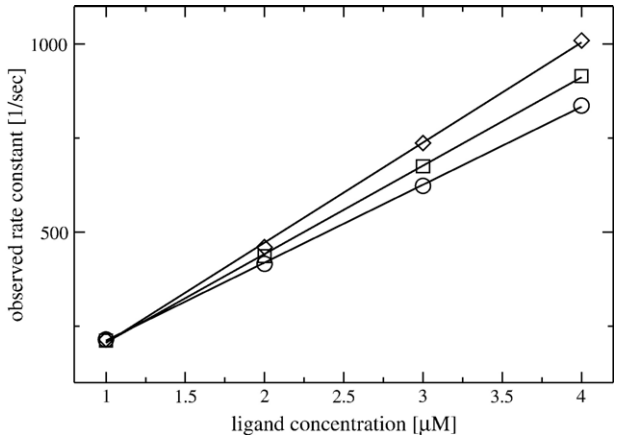

Fig. 4. Dependencies of the observed rate constants, k_{obs} on the concentration of m^7GpppG for the experimental conditions close to those employed by Slepenkov and coworkers [14]. All three sets of parameters of the two-step binding model shown in Table 2 for m^7GpppG were used in simulation of the kinetic traces: experiment 1 — circles; experiment 2 — squares; experiment 3 — diamonds.

[10,13] and by Slepenkov and coworkers [14]. The first group concluded a two-step binding mechanism, apparently based on a linear relation between the inverse of the k_{obs} and the inverse of m^7GpppG concentration. However no hyperbolic saturation phenomenon predicted by Eq. (7) was shown by these authors. Therefore, it is not clear for us that the two-step binding mechanism was sufficiently proved. On the other hand, Slepenkov and coworkers performed their measurements in a wider concentration range of m^7GpppG, and for several ionic strengths of the solution, and they show that in all cases the relation between k_{obs} and the ligand concentration is linear. Therefore they concluded that the one-step mechanism correctly describes the binding of m^7GpppG by eIF4E protein.

Having in mind the results obtained by Slepenkov and coworkers for human eIF4E and m^7GpppG, one may ask if the experimental observations of those authors are in contradiction to the results of our work. To answer this question we simulated, using the DynaFit program, kinetic transients analogous to those obtained by Slepenkov and coworkers. The script file used for these simulations is similar to one presented in reference [29]. We simulated kinetic transients for ionic strength of 150 mM, and for 4 concentrations of m^7GpppG, for each set of two-step model parameters shown in Table 2 for this cap analogue. Each simulated kinetic transient was fitted with mono-exponential function, represented by Eq. (4), resulting in a value of the observed rate constant, k_{obs}, corresponding to a given concentration of the ligand. Three resulting dependencies of k_{obs} on the ligand concentration are shown if Fig. 4. It can be seen that all three dependencies are strictly linear in the investigated range of the ligand concentrations. This concentration range satisfies requirements of the pseudo-first order reaction condition which justifies fitting of mono-exponential functions, and corresponds to the concentration range for data with 150 mM added KCl shown in Fig. 3A of Slepenkov and coworkers [14]. Therefore, we should conclude that the linear dependence of the k_{obs} versus ligand concentration obtained from stopped-flow experiments under pseudo-first order reaction conditions does not prove that the binding is a one-step reaction. The rate constants obtained from our two-step binding model do not justify approximations used in derivation of Eq. (7).

3.4. Conclusions

Taking together the results of the model selection analysis, and the linear dependencies of the observed rate constant on the ligand concentration for the simulated stopped-flow transients, described above, we obtain a reliable conclusion that binding of cap analogues by the eukaryotic initiation factor 4E is at least a two-step binding process. Structural changes occurring within eIF4E protein upon cap binding were suggested almost 20 years ago on the basis of circular dichroism and fluorescence studies [32]. The $^{15}N/^{1}H$ correlated NMR spectra of eIF4E in the apo form and in the presence of m^7GDP were interpreted as indicating that cap binding induces the transition of mostly unfolded eIF4E to a folded state [33]. However, a very recent report of the first cap-free eIF4E structure demonstrated that the apo form of eIF4E is also structured in the absence of the cap, although it confirmed substantial conformational changes upon binding of the ligand [34]. The structural changes in eIF4E upon cap binding influences interactions of eIF4E protein with other molecular factors involved in the initiation of translation. For example they provide a mechanism for the enhanced affinity of adaptor protein eIF4G for the eIF4E–cap complex relative to the apo form [33,34]. Our present study provides evidences that occurrence of these structural changes is reflected in the kinetics of the cap binding to the eIF4E protein.

Acknowledgements

We thank Dr. J. Zuberek for the preparation samples of murine eIF4E protein, Dr. Petr Kuzmic for the helpful discussions, and Dr. Joanna Trylska for reading the manuscript. All plots were done using program xmgrace (Evgeny Stambulchik, Rehovot, Israel).

References

[1] A.J. Shatkin, Capping of eukaryotic mRNAs, Cell 9 (1976) 645–653.
[2] N. Sonenberg, mRNA 5′ cap-binding protein eIF4E and control of cell growth, in: J. Hershey, M.B. Mathews, N. Sonenberg (Eds.), Translation Control, Cold Spring Harbor Laboratory Press, New York, 1996, pp. 245–269.
[3] T.V. Pestova, J.R. Lorch, C.U.T. Hellen, The mechanism of translation initiation in eukaryotes, in: M.B. Mathews, N. Sonenberg, J. Hershey (Eds.), Translation Control in Biology and Medicine, Cold Spring Harbor Laboratory Press, New York, 2007, pp. 87–128.
[4] J. Marcotrigiano, A. Gingras, N. Sonenberg, S.K. Burley, Cocrystal structure of the messenger RNA 5′ cap-binding protein (eIF4E) bound to 7-methyl-GDP, Cell 89 (1997) 951–961.
[5] A. Niedźwiecka, J. Marcotrigiano, J. Stępiński, M. Jankowska-Anyszka, A. Wysłouch-Cieszyńska, M. Dadlez, A. Gingras, P. Mak, E. Darżynkiewicz, N. Sonenberg, S.K. Burley, R. Stolarski, Biophysical studies of eIF4E cap-binding protein: recognition mRNA 5′ cap structure and synthetic fragments of eIF4G and 4E-BP1 proteins, J. Mol. Biol. 319 (2002) 615–635.
[6] K. Tomoo, X. Shen, K. Okabe, Y. Nozoe, S. Fukuhara, S. Morino, M. Sasahi, T. Taniguchi, H. Miygawa, K. Kitamura, K. Miura, T. Ishida, Structural features of human initiation factor 4E studied by X-ray crystal analysis and molecular dynamics simulations, J. Mol. Biol. 328 (2003) 365–383.

[7] H. Matsuo, H. Li, A.M. McGuire, C.M. Fletcher, A. Gingras, N. Sonenberg, G. Wagner, Structure of translation factor eIF4E bound to m7GDP and interaction with 4E-binding protein, Nat. Struct. Biol. 4 (1997) 717–724.
[8] S.E. Carberry, R.E. Rhoads, D.J. Goss, A spectroscopic study of binding of m^7GTP and m^7GpppG to human protein synthesis initiation factor 4E, Biochemistry 28 (1989) 8078–8082.
[9] A. Cai, M. Jankowska-Anyszka, A. Centers, L. Chlebicka, J. Stepinski, R. Stolarski, E. Darzynkiewicz, R.E. Rhoads, Quantitative assessment of mRNA cap analogs as inhibitors of in vitro translation, Biochemistry 38 (1999) 8538–8547.
[10] M. Sha, Y. Wang, T. Xiang, A. van Heerdens, K.S. Browning, D.J. Goss, Interaction of wheat germ protein synthesis initiation factor eIF-(*iso*)4F and its subunits p28 and p86 with m^7GTP and mRNA analogues, J. Biol. Chem. 270 (1995) 29904–29909.
[11] E. Błachut-Okrasińska, E. Bojarska, A. Niedźwiecka, L. Chlebicka, E. Darżynkiewicz, R. Stolarski, J. Stępiński, J.M. Antosiewicz, Stopped-flow and Brownian dynamics studies of electrostatic effects in the kinetics of binding of 7-methyl-GpppG to the protein eIF4E, Eur. Biophys.J. 29 (2000) 487–498.
[12] M. Długosz, E. Błachut-Okrasińska, E. Bojarska, E. Darżynkiewicz, J.M. Antosiewicz, Effects of pH on kinetics of binding of mRNA-cap analogs by translation initiation factor eIF4E, Eur. Biophys. J. 31 (2003) 608–616.
[13] M.A. Khan, D.J. Goss, Translation initiation factor (eIF) 4B affects the rates of binding of the mRNA m^7G cap analogue to wheat germ eIFiso4F and eIFiso4F●PABP, Biochemistry 44 (2005) 4510–4516.
[14] S.V. Slepenkov, E. Darzynkiewicz, R.E. Rhoads, Stopped-flow kinetic analysis of eIF4E and phosphorylated eIF4E binding to cap analogs and capped oligoribonucleotides, J. Biol. Chem. 281 (2006) 14927–14938.
[15] K.A. Johnson, Transient-state kinetic analysis of enzyme reaction pathways, Enzymes 20 (1992) 1–61.
[16] S. Strickland, G. Palmer, V. Masey, Determination of dissociation constants and specific rate constants of enzyme–substrate (or protein–ligand) interactions from rapid reaction kinetic data, J. Biol. Chem. 250 (1975) 4048–4052.
[17] S.G. Rhee, P.B. Chock, Mechanistic studies of glutamine synthetase from *Escherichia coli*: kinetics of ADP and orthophosphate binding to the unadenylated enzyme, Biochemistry 15 (1976) 1755–1760.
[18] D.L. Garland, Kinetics and mechanism of colchicine binding to tubulin: evidence for ligand induced conformational change, Biochemistry 17 (1978) 4266–4272.
[19] C.T. Zimmerle, C. Frieden, Analysis of progress curves by simulations generated by numerical integration, Biochem. J. 258 (1989) 381–387.
[20] C. Frieden, Analysis of kinetic data: practical applications of computer simulation and fitting programs, Methods Enzymol. 240 (1994) 311–322.
[21] P. Kuzmic, Program DYNAFIT for the analysis of enzyme kinetic data: application to HIV proteinase, Anal. Biochem. 237 (1996) 260–273.
[22] H. Akaike, A new look at the statistical model identification, IEEE Trans. Automat. Contr. 19 (1974) 716–723.
[23] K.P. Burnham, D.R. Anderson, Model Selection and Multimodel Inference: A Practical Information-Theoretic Approach, 2nd edn.Springer-Verlag, New York, 2002.
[24] G. Schwarz, Estimating the dimension of a model, Annals Statistics 6 (1978) 461–464.
[25] B.L. Adams, M. Morgan, S. Muthukrishnan, S.M. Hecht, A.J. Shatkin, The effect of "cap" analogs on reovirus mRNA binding to wheat germ ribosomes, J. Biol. Chem. 253 (1978) 2589–2595.
[26] E. Darżynkiewicz, I. Ekiel, S.M. Tahara, L.S. Seliger, A.J. Shatkin, Chemical synthesis and characterisation of 7-methylguanosine cap analogues, Biochemistry 24 (1985) 1701–1707.
[27] E. Darżynkiewicz, I. Ekiel, P. Lassota, S.M. Tahara, Inhibition of eukaryotic translation by analogues of messenger RNA 5′-cap: chemical and biological consequences of 5′-phosphate modifications of 7-methyl-guanosine of 5′-monophosphate, Biochemistry 26 (1987) 4372–4380.
[28] J. Stępiński, M. Bretner, M. Jankowska, K. Felczak, R. Stolarski, Z. Wieczorek, A. Cai, R.E. Rhoads, A. Temeriusz, D. Haber, E. Darżynkiewicz, Synthesis and properties of P^1,P^{2-}, P^1, P^{3-}, and P^1, P^{4-}, dinucleoside di-, tri- and tertaphosphate mRNA 5′-cap analogues, Nucleosides Nucleotides 14 (1995) 717–721.
[29] P. Kuzmic, A generalized numerical approach to rapid-equilibrium enzyme kinetics: application to 17β-HSD, Molec. Cell. Endocrinol. 248 (2006) 172–181.
[30] P. Kuzmic, L. Cregar, S.Z. Millis, M. Goldman, Mixed-type noncompetitive inhibition of anthrax lethal factor protease by aminoglycosides, FEBS J. 273 (2006) 3054–3062.
[31] F.J.L. Rodier, G. Ilgenfritz, Two-step interaction of α-chymotrypsin with a fluorescent inhibitor. A dynamic study by the temperature-jump method, Eur. J. Biochem. 128 (1982) 451–454.
[32] W.D. McCubbin, I. Edery, M. Altmann, N. Sonenberg, C.M. Kay, Circular dichroism and fluorescence studies on protein synthesis initiation factor eIF-4E and two mutant forms from the yeast *Saccharomyces cerevisiae*, J. Biol. Chem. 263 (1988) 17663–17671.
[33] T. von der Haar, Y. Oku, M. Ptushkina, N. Moerke, G. Wagner, J.D. Gross, J.E.G. McCarthy, Folding transitions during assembly of the eukaryotic mRNA cap-binding complex, J. Mol. Biol. 356 (2006) 982–992.
[34] L. Volpon, M.J. Osborne, I. Topsisirovic, N. Siddiqui, K.L.B. Borden, Cap-free structure of eIF4E suggests a basis for conformational regulation by its ligands, EMBO J. 25 (2006) 5138–5149.